Applied Physics Letters

Femtosecond laser direct writing continuous phase vortex gratings with proportionally distributed diffraction energy

Cite as: Appl. Phys. Lett. **119**, 131101 (2021); https://doi.org/10.1063/5.0061590
Submitted: 28 June 2021 • Accepted: 08 September 2021 • Published Online: 27 September 2021

Liqun Xu, Chaowei Wang, Xinbo Qi, et al.

Applied Physics Letters ARTICLE scitation.org/journal/apl

Femtosecond laser direct writing continuous phase vortex gratings with proportionally distributed diffraction energy

Cite as: Appl. Phys. Lett. **119**, 131101 (2021); doi: 10.1063/5.0061590
Submitted: 28 June 2021 · Accepted: 8 September 2021 ·
Published Online: 27 September 2021

Liqun Xu,[1] Chaowei Wang,[1,a)] Xinbo Qi,[1] Rui Li,[1] Chenchu Zhang,[2] Leran Zhang,[1] Zhongguo Ren,[1] Zihang Zhang,[1] Jiawen Li,[1] Yanlei Hu,[1] Dong Wu,[1,a)] and Jiaru Chu[1]

AFFILIATIONS

[1]Hefei National Laboratory for Physical Sciences at the Microscale and CAS Key Laboratory of Mechanical Behavior and Design of Materials, Department of Precision Machinery and Precision Instrumentation, University of Science and Technology of China, Hefei 230026, China

[2]Anhui Province Key Lab of Aerospace Structural Parts Forming Technology and Equipment, Institute of Industry and Equipment Technology, Hefei University of Technology, Hefei 230009, China

[a)]**Authors to whom correspondence should be addressed:** chaoweiw@ustc.edu.cn and dongwu@ustc.edu.cn

ABSTRACT

In this Letter, we propose a type of continuous phase vortex gratings (CPVGs), which are able to generate a series of vortex beams with equal or proportional diffracted energies and different topological charges (TCs). A set of CPVGs with dimensions ($60 \times 60 \times 1.1\ \mu m^3$) are directly designed by mathematical equations, which avoids the use of iterative algorithms. The CPVGs are fabricated by femtosecond laser direct writing (FsLDW) with photoresist, and the experimentally generated vortex beams are in good agreement with the theoretical designs, exhibiting high optical efficiencies. In addition, we realized a CPVG onto the tip of a composite fiber for integrated optical systems. Our work paves the way for applications in optical communications, optical manipulations, and high-performance integrated optics.

A fundamental property of light is to rotate when traveling in space. The common form of such rotation is polarized rotation, or spin angular momentum (SAM) carried by photons of light which have two possible quantized values of $\pm\hbar$. In 1992, Allen *et al.*[1] proposed that light has another form of angular momentum, known as orbital angular momentum (OAM), which can be derived from its helical wavefront structure $\exp(il\phi)$, where l is the topological charge (TC) and ϕ is the azimuthal angle. Considering momentum circulates around the optical axis, the OAM beams are also called vortex beams, which have a phase singularity at the center of the optical axis, resulting in zero intensity on the axis. Therefore, the vortex beams exhibit a donut shaped intensity pattern. The vortex beams with OAM have been extensively used in high-density information storage and transmission[2] and optical wrenches.[3]

So far, researchers have obtained vortex beams in different ways, including, but not limited to, spiral phase plates,[4] q-plates,[5,6] spatial light modulators(SLMs),[7] metasurfaces,[8,9] vortex gratings,[10,11] and so on.[12,13] The general results of these investigations have provided a powerful tool for further studies of the optical vortices, which has created a new chapter of modern optics. Using vortex gratings for the generation of vortex beams is a particularly simple and efficient method, which can provide a series of vortices carrying different TCs without a complex experimental system. For some applications, given that optical components need to be miniaturized and integrated into systems containing additionally electrical, mechanical, or other optical components, and the miniaturization of lenses is limited, diffractive elements like gratings hold tremendous advantages. However, the energy distribution of vortex beams generated by transitional vortex gratings is not uniform, and the zero-order always occupies most of the energy while the higher orders decay so rapidly that they cannot be detected in practice. While in the applications mentioned above, it is usually desirable to concentrate as much energy as possible into certain specified orders and ensure that the energy is divided evenly, or more generally, in a specific proportion.

Some methods have been proposed to address this problem. The Dammam vortex grating (DVG) draws the attention of researchers because it provides a convenient method for generating a large number of vortex beams with identical intensities and different TCs.[14]

Recently, Wang *et al.*[15] have used genetic algorithm (GA) to optimize the positions of the phase transitional points of the DVG, which could achieve the concentration of the diffracted energy on certain orders. However, their practical implementations have been restricted only to binary gratings, because the manufacturing techniques they used cannot obtain complex "wavy" surfaces. The fabricated binary gratings can only obtain equi-intense optical vortices with spatial symmetry with respect to the optical axis, and each target light field requires a separate iterative process to achieve. As a result, the design of vortex gratings, which can produce vortex beams with asymmetric intensities in the various diffracted orders, is still in high demand.

In this Letter, based on the design theory of phase-only optimal beam splitting developed by Romero *et al.*,[16,17] we design continuous phase gratings encoded with helical phases without the use of iterative algorithms. Femtosecond laser direct writing (FsLDW) by two-photon polymerization (TPP),[18] as an unprecedented and powerful technique enabling 3D fabrication of numerous photonic structures and devices, is adopted to fabricate the grating patterns calculated through the analytical formula. The continuous phase vortex grating (CPVG) with length (60 μm) and height (1.1 μm) is capable of simultaneously generating multiple vortices with different TCs at different diffracted orders in far field. By adjusting a set of numerical parameters of the transmission function of the CPVG, certain diffracted orders can be selectively suppressed or enhanced. We should emphasize that the biggest advantage of our design is its versatility, which allows for the asymmetrical energy distribution of the target diffracted orders. In addition, we fabricated a CPVG on the tip of a composite fiber, which avoids the use of bulky illumination light paths, and paves the way for the applications of CPVGs in micro-optical systems.

The vortex grating can be considered as a type of computer generating hologram (CGH),[19] and its transmission function where a helical phase is embedded can be expressed as

$$T(x,y) = \sum_{m=-\infty}^{\infty} A_m \exp\left[im(2\pi x/\Lambda + l \times arctan(y/x))\right]. \quad (1)$$

Here, A_m represents the component of each diffracted order, $|A_m|^2$ represents the intensity of the m-order vortex beam, (x, y) are the Cartesian coordinates in the plane of the grating, and l is the basic TC. When we choose $l = 0$, the vortex grating becomes a one-dimensional linear grating, and Λ is the corresponding period. From Eq. (1), we can find that if l is a non-zero value, the TC carried by the m-order vortex beam is m $\times$ l. Thus, the CPVG can generate a series of vortex beams with different TCs. Equation (1) is equivalent to

$$T(x,y) = P(x,y) + iQ(x,y), \quad (2)$$

where

$$P(x,y) = \sum_{m\in M} A_m \cos\left[m(2\pi x/\Lambda + l \times arctan(y/x))\right] \quad (3)$$

$$Q(x,y) = \sum_{m\in M} A_m \sin\left[m(2\pi x/\Lambda + l \times arctan(y/x))\right]. \quad (4)$$

Thus, the phase structure of CPVG can be written as

$$\varphi(x,y) = \tan^{-1}\left[Q(x,y)/P(x,y)\right]. \quad (5)$$

If the energy is expected to be concentrated on some specific diffracted orders, the only thing we need to do is to decrease the values of diffracted components outside these specific orders as much as possible. Therefore, the process of proportionally distributing the diffracted energy to the specified orders can be directly realized by a mathematical method. It is worth noting that symmetry is not necessary for continuous phase gratings, so we can selectively eliminate or enhance arbitrary orders to produce an asymmetric pattern of diffracted orders. In our experiment, the loaded basic TC in the CPVG is $l = 1$, for example. According to the required diffracted energy distribution, we adjust the diffracted component of each order in Eq. (1) and then use Eq. (5) to directly obtain the phase structure of the corresponding vortex grating. The result shown in Fig. 1(b) is a 600 $\times$ 600 pixel CGH calculated according to the phase information.

In order to fabricate the CPVG, the CGH needs to be converted into a height profile. It is known that the relation between the thickness and phase is

$$h(x,y) = \lambda_{in}\varphi(x,y)/[2\pi(n_m - 1)], \quad (6)$$

where λ_{in} is the wavelength of incident light for generating vortex beams and n_m represents the refractive indices of photoresist [SZ2080 (IESL-FORTH)] mixed with 1 wt. % 4,4-bis(diethylamino)benzophenone (BIS) as photoinitiator with absorption maximum at 368 nm (Sigma-Aldrich GmbH), which has a low shrinkage and high optical transmissivity and is widely used for micro-optical elements. In our experiment, a green laser with a wavelength of 532 nm is selected as the light source, and the refractive index of photoresist is ~1.5. The CPVG after height conversion is shown in Fig. 1(c). Due to the precision (~100 nm) of our FsLDW system [Fig. 1(a)], the height of the CPVG is segmented with a step of 100 nm. Our fabrication is carried out layer by layer, which causes the CPVG to be divided into 11 layers. The height is discretized according to the following principle:

$$h = \begin{cases} 0, & 0 \le h < 50 \\ 100i\,\text{nm}, & 50 + 100(i-1) \le h < 50 + 100i \\ 1100\,\text{nm}, & 1050 \le h \le 1100. \end{cases} \quad (7)$$

The CPVG was fabricated by focusing the femtosecond laser beam (Coherent Chameleon Vision-S, 80 MHz repetition rate, 800 nm center wavelength, and 75 fs pulse width) into the photoresist using a 60$\times$ oil immersion objective lens with a numerical aperture (NA) of 1.35, and the exposing power was set to be 8.5 mW. The fabrication process of the x–y plane was realized by a pair of scanning galvo mirrors, while the movement between layers was controlled by a vertical precision z positioner. In the process of unpolymerized resin rinsing, the step-like surface tends to be smooth due to the self-smoothing effect, resulting in the continuous phase distribution of the whole CPVG. The scanning electron microscope (SEM; FEI Sirion200) image manifests the high processing quality of the FsLDW, as shown in Fig. 1(d).[20]

Given that the surface morphology of the CPVG is a significant factor in our fabrication, the topography of the CPVG was characterized by an atomic force microscope (AFM; Dimension Icon, Bruker, CA) with a PPP-FM probe (NANOSENSORS, Switzerland) in a tapping mode. The CPVG is processed on a substrate with a height of 500 nm to ensure the integrity of the phase, so the maximum height is 1.6 μm. The height profile of the CPVG relative to the substrate extracted along the horizontal line marked in Fig. 1(e) is shown in Fig. 1(f), which indicates that the height extracted by AFM has a good

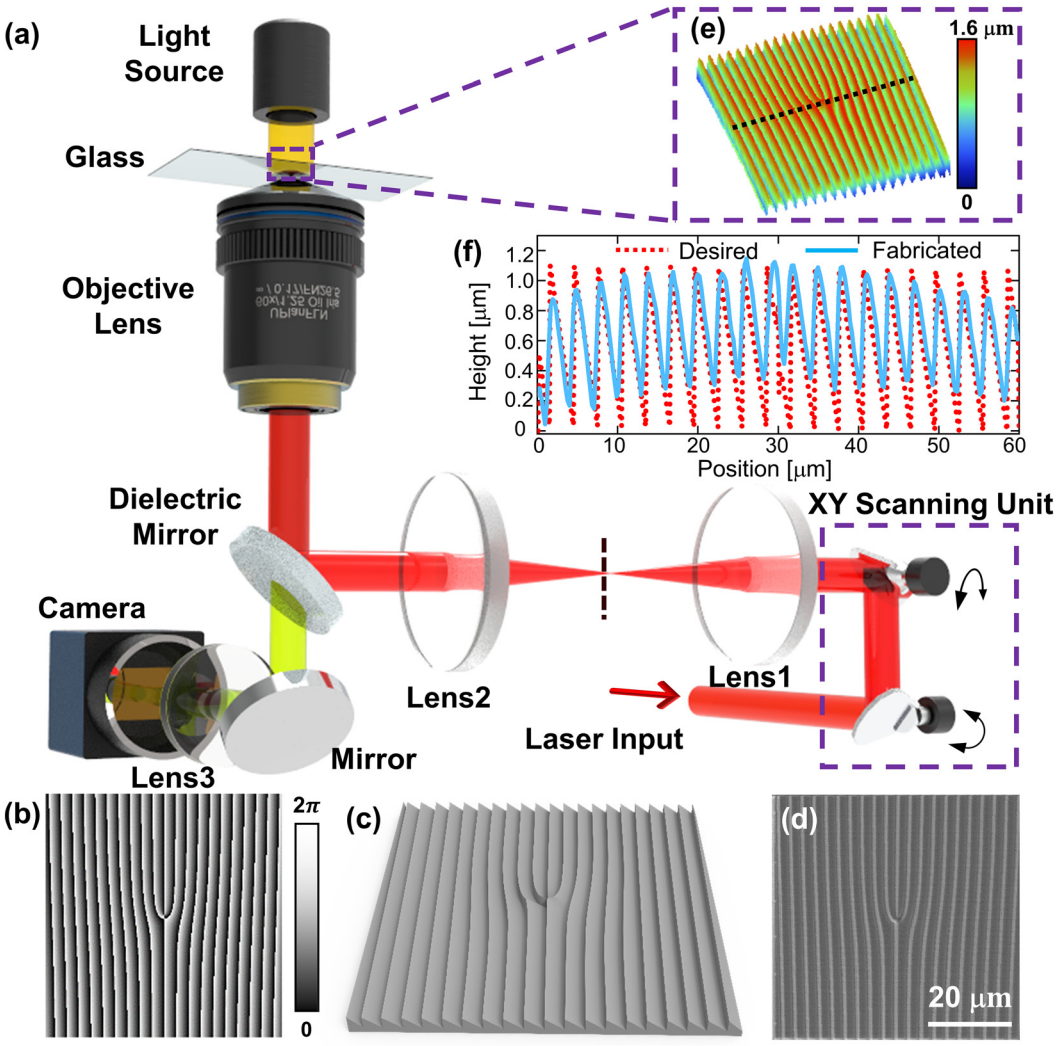

FIG. 1. Fabrication of the continuous phase vortex gratings (CPVGs) by femtosecond laser direct writing (FsLDW). (a) Schematic diagram of the experimental setup for the fabrication of the CPVGs. (b) Phase pattern of a CPVG wrapped between 0 and 2π. Size, 600×600 pixels. (c) The ideal three-dimensional (3D) CPVG after the height conversion. (d) SEM micrograph of the fabricated CPVG. (e) 3D AFM image of the fabricated CPVG. (f) Height profile with respect to the substrate (500 nm) along the black line shown in (e). The solid line represents the extracted profile, while the dashed line represents the designed profile.

agreement with the designed value. Some small differences between the designed and the measured height profile may be caused by fabrication or measurement errors. Since some local structures are close to the fabrication precision in the up and bottom of the grating, some mismatches are unavoidable during fabrication and development. It should also be noted that due to the high aspect ratio of the local areas, the AFM probe cannot dip into the bottom, which causes the mismatch between the designed height and the extracted height in the corner of the CPVG.[21]

We choose to demonstrate that the energy is evenly distributed ($\pm$3rd orders, or $-$1st and $+$2nd orders, respectively), or distributed at the ratio of 1:2 in two diffracted orders ($-$3rd and $+$3rd orders, or $-$1st and $+$3rd orders, respectively). The designed phase patterns are shown in Figs. 2(a-1)–2(d-1). Then, we fabricate and characterize a series of CPVGs, which produce numerous vortex beams with symmetric or asymmetric intensities in the specified diffracted orders, as shown in Figs. 2(a-2)–2(d-2) and Figs. 2(a-3)–2(d-3), respectively. In the first case, phase structure $\varphi(x, y)$ is subjected to the constraint that $|A_{-3}| = |A_{+3}|$. Now Eq. (3) gives us $\varphi(x, y) = \tan^{-1}(0)$, i.e., the phase of the CPVG with the energy being symmetrically concentrated in the $\pm$3-order vortex beams has only two results, 0 or π, which is a special case of the CPVGs.

In order to characterize the performance of the CPVGs, a series of tests have been carried out. A $10\times$ objective lens (NA = 0.25) was used to focus the laser onto the sample, and the diffracted patterns were captured by a CCD camera. Figure 3 is a comparison between the theoretical models and the experimental results, which displays the far-field diffracted patterns and the normalized energy distribution of

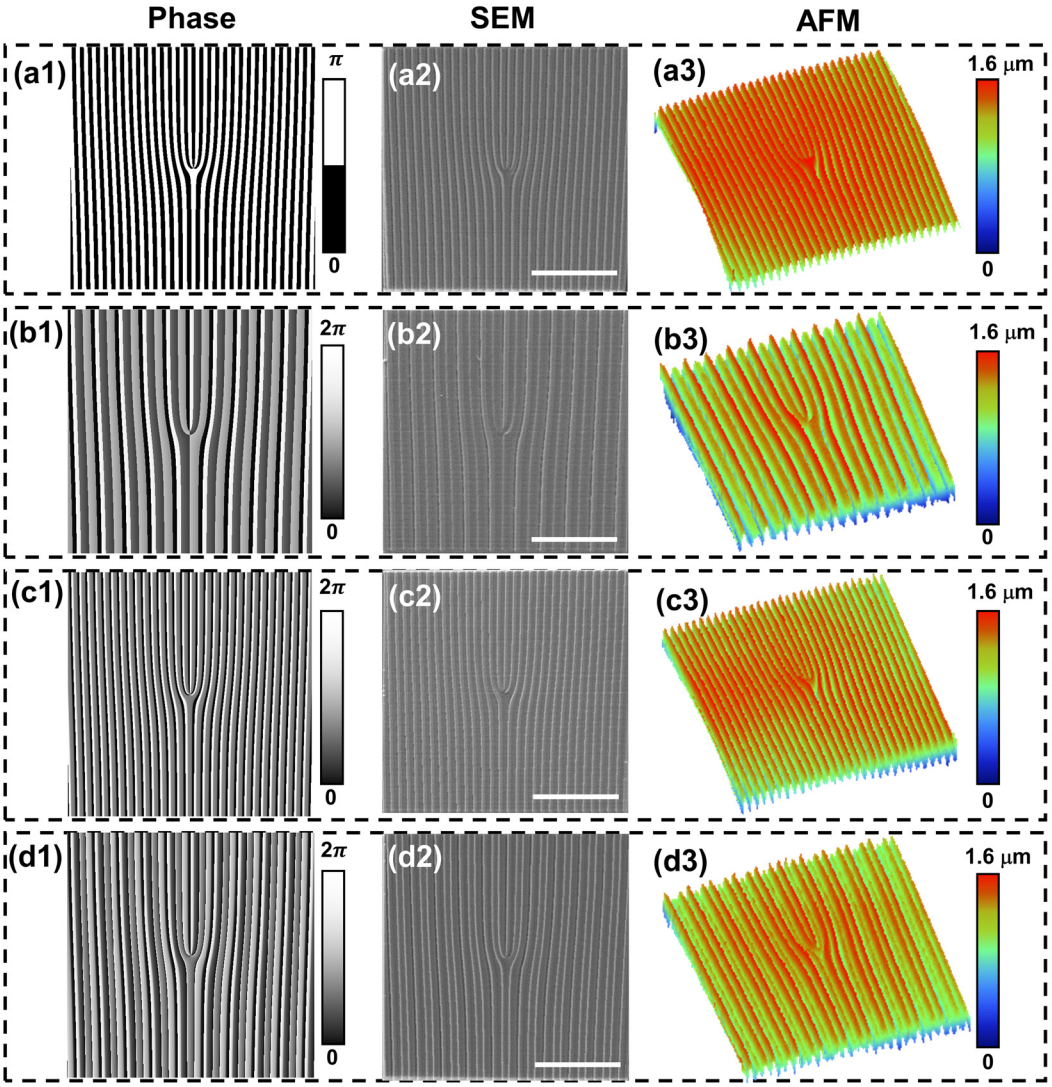

FIG. 2. Fabrication and characterization of a set of CPVGs. (a-1)–(d-1) Phase patterns of the CPVGs with the energy being evenly distributed (a1) in the ±3rd orders, or (b1) in the −1st and the +2nd orders, and unevenly distributed (c1) in the −3rd and the +3rd orders, or (d1) in the −1st and the +3rd orders with the ratio of 1:2. (a-2)–(d-2) SEM and (a-3)–(d-3)3D AFM images of the fabricated CPVGs correspond to (a-1)–(d-1), respectively. All scale bars: 20 μm.

each diffracted order. As expected, in the first case, the majority of the power is concentrated in the ±3rd orders. As we choose $l = 1$, the output ±3-order vortex beams carry TCs of ±3, which is in accordance with Eq. (1). Afterward, two strong −1st and +2nd orders occupying the most energy and carrying the TCs of −1 and +2 are achieved in the next case. Similarly, the energy is sent to the −3rd and the +3rd orders, or the −1st and the +3rd orders with the ratio around 1:2 (TCs are (−3, +3) and (−1, +3), respectively) by the CPVGs. It can be seen that the experimental results are in good agreement with the theoretical models.

The potential of the CPVGs depends to a great extent on their optical efficiency, which is defined as the fraction of the total energy diffracted into a desired order.[22] The optical efficiencies of the CPVGs are estimated to be ∼92% (orders: −3rd, +3rd; ratio: 1:1), ∼80% (orders: −1st, +2nd; ratio: 1:1), ∼90% (orders: −3rd, +3rd; ratio: 1:2), and ∼79% (orders: −1st, +3rd; ratio: 1:2), respectively. The experimental results exhibit the high optical efficiencies of our fabricated CPVGs. Some considerations must be taken in the experimental results. The CGHs are pixelated devices, so the designed continuous phase profile is not exactly replicated. On the other hand, there are inevitable errors during the manufacturing and developing process, which ultimately leads to some undesired diffracted orders that cannot be completely suppressed.

The CPVG can easily generate specified vortex beams with the use of optical fibers, which are widely utilized in the manipulation of micro-optical systems due to their inherent flexibility and

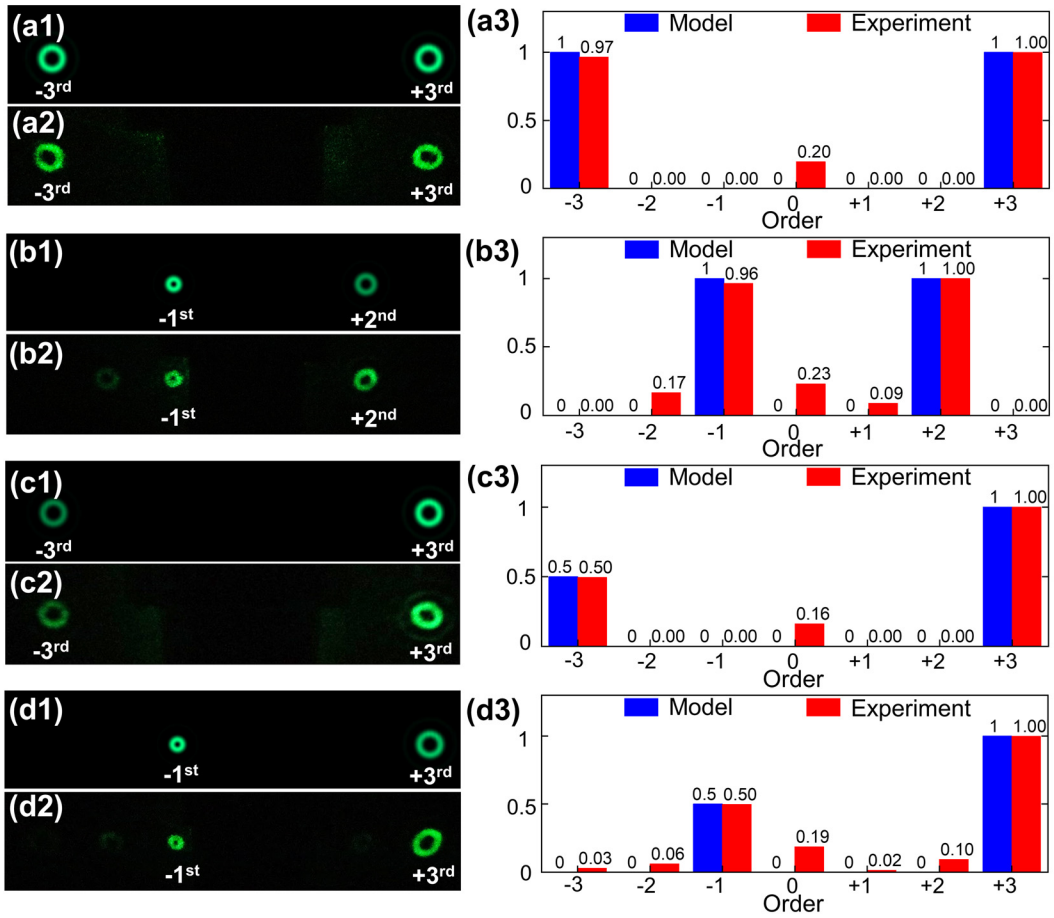

FIG. 3. Comparisons between the theoretical models and the experimental results of the CPVGs with specified diffracted energy distribution. (a-1)–(d-1) Simulated diffraction patterns of the CPVGs shown in Figs. 2(a-1)–2(d-1), respectively. (a-2)–(d-2) Measured diffraction patterns of the CPVGs. The zero diffraction orders are blocked for clarity. (a-3)–(d-3) Comparisons between the theoretical models and the experimental results of the normalized energy distribution of each diffracted order shown in (a-1)–(d-1) and (a-2)–(d-2), respectively. The blue pillars represent the theoretical models, while the red pillars represent the experimental results.

compact configuration without alignment compared with the current used illumination optical systems that suffer from a lack of integrability.[23–27] However, the diameter of the single mode fiber (SMF) core is too small (9 μm) to effectively illuminate the grating (~60 μm size) directly printed on the end face of the SMF. Thus, a 280 μm length of coreless silica fiber (CSF) (Thorlabs, FG125LA) was spliced onto a 7.5 cm length of SMF. As shown in Fig. 4(a), the light from the core of SMF is expanded by concatenating CSF segment, where the output super-Gaussian beam could effectively cover the entire grating.[28] The spread angle θ is determined by the formula

$$NA = n_{CSF} \times \sin\theta, \tag{8}$$

where NA is the numerical aperture of SMF and n_{CSF} is the refractive index of CSF. To achieve splicing of this length of the CSF, we first spliced a longer section of CSF to a SMF and then used an automated glass processor with an in-line cleaver (Thorlabs, Vytran GPX3800) to cleave it into 280 μm.[29] The CPVG with the energy being concentrated in the +2nd-order is directly printed on the far end of the CSF by FsLDW [Fig. 4(b)], and the SEM images shown in Figs. 4(d-1) and 4(d-2) illustrate our precise fabrication of the CPVG at the tip of the fiber. After that, we welded the sample with the test SMF. Figure 4(c) demonstrates the experimental setup for the vortex beams generation from the CPVG integrated at the top face of the composite fiber, from which we can clearly observe that the diffracted energy output from the fiber is mainly concentrated in the +2-order vortex beam, as shown in Fig. 4(e).

In conclusion, we utilize the optimal beam splitting theory proposed by Romero *et al.* into the design of the CPVG, which is capable of converting the incident Gaussian beam into a series of vortex beams and can be conveniently manufactured by FsLDW. Our proposed design method can proportionally distribute the power into arbitrary diffracted orders with the desired TCs, which is in good agreement with the simulated results. Finally, due to the flexibility of femtosecond laser microfabrication, we integrated the designed CPVG onto the top face of a composite fiber, which provides considerable potential for

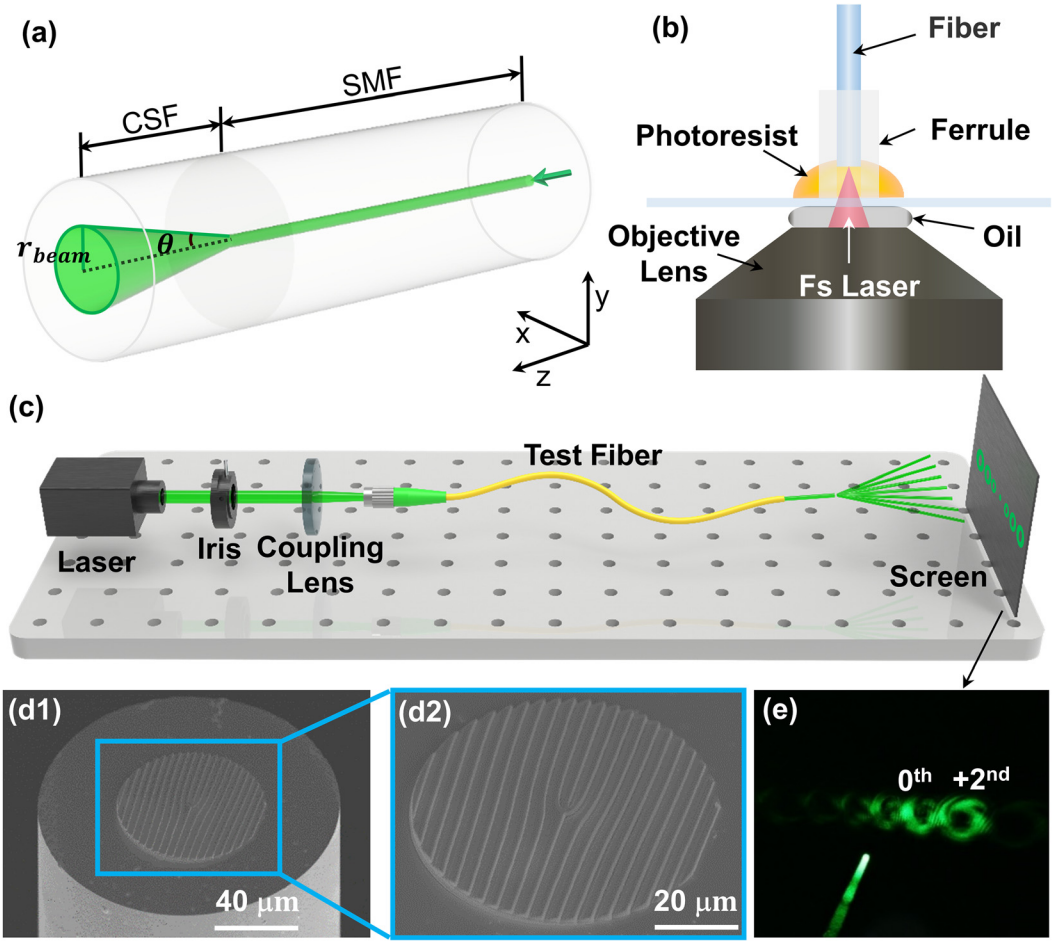

FIG. 4. Integrating a CPVG attached to the tip of a composite fiber. (a) Composite fiber with light exiting the single mode fiber (SMF), expanding in the coreless silica fiber (CSF). (b) Schematic illustration of the printing setup in the FsLDW system. (c) Schematic illustration of the optical performance detection setup. (d1) SEM and (d2) locally magnified SEM images of the fabricated CPVG with the energy being concentrated in the +2nd-order attached to the end facet of an optical fiber. (e) Photograph of the imprinted optical fiber and the realized far-field intensity distribution.

practical applications, such as optical manipulation in miniaturized optical systems.

This work was supported by the National Natural Science Foundation of China (Nos. 61927814, 51875544, and 62005262), Major Scientific and Technological Projects in Anhui Province (No. 201903a05020005), the Fundamental Research Funds for the Central Universities (Nos. JZ2019YYPY0024, PA2020GDSK0077, and WK5290000001), and the China Postdoctoral Science Foundation (Nos. 2020M671888 and 2021T140649). We acknowledge the Experimental Center of Engineering and Material Sciences at USTC for the fabrication and measuring of samples. This work was partly carried out at the USTC Center for Micro and Nanoscale Research and Fabrication. We thank Thorlabs for CSF segment splice and Chengfu Ma for AFM imaging.

DATA AVAILABILITY

The data that support the findings of this study are available from the corresponding author upon reasonable request.

REFERENCES

[1]L. Allen, M. W. Beijersbergen, R. J. C. Spreeuw, and J. P. Woerdman, Phys. Rev. A **45**, 8185 (1992).
[2]X. Fang, H. Ren, and M. Gu, Nat. Photonics **14**, 102 (2020).
[3]M. Padgett and R. Bowman, Nat. Photonics **5**, 343 (2011).
[4]E. Brasselet, M. Malinauskas, A. Žukauskas, and S. Juodkazis, Appl. Phys. Lett. **97**, 211108 (2010).
[5]X. Wang, A. Kuchmizhak, E. Brasselet, and S. Juodkazis, Appl. Phys. Lett. **110**, 181101 (2017).
[6]S. Xu, H. Fan, S.-J. Xu, Z.-Z. Li, Y. Lei, L. Wang, and J.-F. Song, Nanomaterials **10**, 1737 (2020).
[7]E. Rueda, D. Muñetón, J. A. Gómez, and A. Lencina, Opt. Lett. **38**, 3941 (2013).

[8]E. Karimi, S. A. Schulz, I. D. Leon, H. Qassim, J. Upham, and R. W. Boyd, Light: Sci. Appl. **3**, e167 (2014).
[9]M. Q. Mehmood, S. Mei, S. Hussain, K. Huang, S. Y. Siew, L. Zhang, T. Zhang, X. Ling, H. Liu, J. Teng, A. Danner, S. Zhang, and C. W. Qiu, Adv. Mater. **28**, 2533 (2016).
[10]N. R. Heckenberg, R. McDuff, C. P. Smith, and A. G. White, Opt. Lett. **17**, 221 (1992).
[11]A. Y. Bekshaev and A. I. Karamoch, Opt. Commun. **281**, 1366 (2008).
[12]E. Brasselet, A. Royon, and L. Canioni, Appl. Phys. Lett. **100**, 181901 (2012).
[13]S. S. Fedotov, R. Drevinskas, S. V. Lotarev, A. S. Lipatiev, M. Beresna, A. Čerkauskaitė, V. N. Sigaev, and P. G. Kazansky, Appl. Phys. Lett. **108**(7), 071905 (2016).
[14]N. Zhang, X. C. Yuan, and R. E. Burge, Opt. Lett. **35**, 3495 (2010).
[15]H. Wang, D. Wei, X. Xu, M. Wang, G. Cui, Y. Lu, Y. Zhang, and M. Xiao, Appl. Phys. Lett. **113**, 221101 (2018).
[16]L. A. Romero and F. M. Dickey, J. Opt. Soc. Am. A **24**, 2280 (2007).
[17]L. A. Romero and F. M. Dickey, Prog. Opt. **54**, 319 (2010).
[18]L. Jonušauskas, S. Juodkazis, and M. Malinauskas, J. Opt. **20**, 053001 (2018).
[19]L. Janicijevic and S. Topuzoski, J. Opt. Soc. Am. A **25**, 2659 (2008).
[20]Z. Cai, Y. Liu, C. Zhang, J. Xu, S. Ji, J. Ni, J. Li, Y. Hu, D. Wu, and J. Chu, Opt. Lett. **42**, 2483 (2017).
[21]Z. Cai, Y. Liu, Y. Hu, C. Zhang, J. Xu, S. Ji, J. Ni, Z. Lao, J. Li, Y. Zhao, and D. Wu, Opt. Lett. **43**, 1151 (2018).
[22]J. Albero, J. A. Davis, D. M. Cottrell, C. E. Granger, K. R. McCormick, and I. Moreno, Appl. Opt. **52**, 3637 (2013).
[23]T. Gissibl, M. Schmid, and H. Giessen, Optica **3**, 448 (2016).
[24]T. Gissibl, S. Thiele, A. Herkommer, and H. Giessen, Nat. Commun. **7**, 11763 (2016).
[25]T. Gissibl, S. Thiele, A. Herkommer, and H. Giessen, Nat. Photonics **10**, 554 (2016).
[26]K. Weber, F. Hütt, S. Thiele, T. Gissibl, A. Herkommer, and H. Giessen, Opt. Express **25**, 19672 (2017).
[27]S. Schmidt, S. Thiele, A. Toulouse, C. Bösel, T. Tiess, A. Herkommer, H. Gross, and H. Giessen, Optica **7**, 1279 (2020).
[28]S. Kang, H. Joe, J. Kim, Y. Jeong, B. Min, and K. Oh, Appl. Phys. Lett. **98**, 241103 (2011).
[29]J. Li, S. Thiele, B. C. Quirk, R. W. Kirk, J. W. Verjans, E. Akers, C. A. Bursill, S. J. Nicholls, A. M. Herkommer, H. Giessen, and R. A. McLaughlin, Light: Sci. Appl. **9**, 124 (2020).